

# Simulation of High-Efficiency Crystalline Silicon Solar Cells With Homo–Hetero Junctions

Sihua Zhong, Xia Hua, and Wenzhong Shen

**Abstract**—A novel solar cell structure consisting of both homojunction and heterojunction (homo–hetero junctions), which possesses a potential to realize high photoelectric conversion efficiency, is investigated by the numerical simulation tool AFORS-HET. We demonstrate that the homo–hetero junctions solar cell has a higher fill factor than the solar cell with heterojunction with intrinsic thin layer (HIT), due to the reduced series resistance, which results in a better conversion efficiency, whereas their interfacial density of states (DOS) values are identical. Through a detailed study of the effect of inserting a homojunction, we find that the field-effect passivation can adequately explain the interesting behaviors that the open-circuit voltage increases and the emitter saturation current density declines when increasing the doping concentration in the P-type crystalline silicon layer. In addition, as compared with the HIT solar cell, the homo–hetero junctions solar cell is less sensitive to the DOS due to the field-effect passivation, leading to a comparable open-circuit voltage even if its total interfacial DOS is 10 times higher.

**Index Terms**—AFORS-HET, high efficiency, homo–hetero junctions, interfacial recombination, solar cell.

## I. INTRODUCTION

CONSIDERABLE interest exists for silicon heterojunction solar cells due to their potential of achieving high conversion efficiency at low cost. Generally, a thin layer of intrinsic hydrogenated amorphous silicon (I-a-Si:H) which has excellent surface passivation is inserted between a crystalline silicon (c-Si) substrate and a heavily doped amorphous silicon [1]–[3]. It is often referred to as heterojunction with intrinsic thin layer (HIT). Sanyo, now Panasonic, has well developed this kind of solar cells and promoted the conversion efficiency as high as 24.7%. Several famous groups also do good works on heterojunction solar cells [4]–[11], and their results have contributed to the better understanding of the physical and technological aspects of silicon heterojunction solar cells. Despite the passivation effect of I-a-Si:H, the introduction of an intrinsic thin layer of a-Si also results in negative effects due to its high resistivity, which will decrease the fill factor (FF)

Manuscript received February 3, 2013; revised March 31, 2013 and April 18, 2013; accepted April 21, 2013. Date of publication May 23, 2013; date of current version June 17, 2013. This work was supported in part by the National Major Basic Research Project 2012CB934302 and Project 2011AA050502, and Natural Science Foundation of China under Grant 11074169, Grant 11174202, and Grant 61234005. The review of this paper was arranged by Editor A. G. Aberle.

The authors are with the Institute of Solar Energy, the Key Laboratory of Artificial Structures and Quantum Control (Minister of Education), Department of Physics, Shanghai Jiao Tong University, Shanghai 200240, China (e-mail: zhongsh@sjtu.edu.cn; huax@sjtu.edu.cn; wzshen@sjtu.edu.cn).

Color versions of one or more of the figures in this paper are available online at <http://ieeexplore.ieee.org>.

Digital Object Identifier 10.1109/TED.2013.2259830

of solar cells [12]–[14], and great sensitivity to the interfacial density of states (DOS) [15]. Therefore, it is significant to find a new passivation layer to replace the I-a-Si:H layer, which can enhance FF while preserving comparable passivation effect.

It is well known that N/N<sup>+</sup> and P/P<sup>+</sup> homojunctions are often used as field-effect passivation layers to reduce the recombination rate at back surfaces [16], [17], and some high-efficiency homojunction solar cells also adopt the N/N<sup>+</sup> or P/P<sup>+</sup> junction to passivate the front surfaces [18]. The field-effect passivation has also been utilized in the high-efficiency multilayer tandem solar cell with a parallel connection of N<sup>+</sup>/N/N<sup>−</sup>/I/P<sup>−</sup>/P/P<sup>+</sup>, exhibiting more efficiency to separate photon-generated carriers as compared with the traditional tandem solar cell connected in series, due to the same electric field direction over the whole cell structure [19]. In order to reduce the recombination at the interface of a heterojunction solar cell, Nils-Peter Harder [20] has proposed a novel solar cell structure comprising of both homojunction and heterojunction (homo–hetero junctions). With an attempt to better understand the benefit of the homo–hetero junctions solar cell, in this paper, we have investigated the physical aspects and properties of a homo–hetero junctions solar cell with the structure of P<sup>+</sup>-a-Si/P-c-Si/N-c-Si substrate/N<sup>+</sup>-a-Si by utilizing the AFORS-HET software as the numerical simulation tool, which was developed by Helmholtz-Zentrum Berlin. We have demonstrated that the FF of the homo–hetero junctions solar cell is higher than that of the HIT solar cell owing to the absence of the intrinsic layer. When the interfacial DOS is low enough, both the HIT and homo–hetero junctions solar cells hold almost the same high open-circuit voltage, whereas, with the advantage of FF, the homo–hetero junctions solar cell has 1.43% absolute higher conversion efficiency. Furthermore, due to the field-effect passivation from the homojunction, the homo–hetero junctions solar cell possesses a better tolerance for the interfacial DOS.

## II. SIMULATION MODEL

AFORS-HET, based on solving the 1-D Poisson and two carrier continuity equations, is one of the numerical computer simulators that is widely used for studying heterojunction solar cells. In this paper, the structure of the homo–hetero junctions solar cell is P<sup>+</sup>-a-Si/P-c-Si/N-c-Si substrate/N<sup>+</sup>-a-Si, which is shown in Fig. 1. The HIT solar cell is not absolutely a Sanyo-type HIT cell structure, but a structure of P<sup>+</sup>-a-Si/I-a-Si:H/N-c-Si substrate/N<sup>+</sup>-a-Si as the reference system for a

TABLE I  
SIMULATION PARAMETERS ADOPTED IN THIS PAPER CB AND VB DENOTE CONDUCTION BAND AND VALENCE BAND, RESPECTIVELY;  
AND A-LIKE AND D-LIKE REPRESENT ACCEPATOR-LIKE AND DONOR-LIKE, RESPECTIVELY

Parameters	P-a-Si:H	I-a-Si:H	N-a-Si:H	N-c-Si	P-c-Si
Layer thickness (cm)	$5 \times 10^{-7}$	$5 \times 10^{-7}$	$5 \times 10^{-7}$	$2.5 \times 10^{-2}$	$0.5 \times 10^{-5}$
Mobility gap (eV)	1.72	1.72	1.72	1.12	variable
Optical gap (eV)	1.72	1.72	1.72	1.12	variable
Donor doping ( $\text{cm}^{-3}$ )	0	0	$7.0 \times 10^{19}$	$1.5 \times 10^{16}$	0
Acceptor doping ( $\text{cm}^{-3}$ )	$7.5 \times 10^{18}$	0	0	0	$1.0 \times 10^{17}$ – $5.0 \times 10^{18}$
Dielectric constant	11.9	11.9	11.9	11.9	11.9
Electronic affinity (eV)	3.90	3.90	3.90	4.05	4.05
Effective DOS in CB ( $\text{cm}^{-3}$ )	$1.0 \times 10^{20}$	$1.0 \times 10^{20}$	$1.0 \times 10^{20}$	$2.84 \times 10^{19}$	variable
Effective DOS in VB ( $\text{cm}^{-3}$ )	$1.0 \times 10^{20}$	$1.0 \times 10^{20}$	$1.0 \times 10^{20}$	$2.68 \times 10^{19}$	variable
Electron (hole) mobility ( $\text{cm}^2/\text{Vs}$ )	20 (5)	20 (5)	20 (5)	1111 (421.6)	variable
Total state density in conduction band ( $\text{cm}^{-3}$ )	$1.6 \times 10^{20}$	$4.0 \times 10^{19}$	$1.4 \times 10^{20}$	—	—
Total state density in valence band ( $\text{cm}^{-3}$ )	$2.4 \times 10^{20}$	$9.0 \times 10^{19}$	$1.9 \times 10^{20}$	—	—
CB tail (VB tail) Urbach energy (eV)	0.037 (0.045)	0.035 (0.050)	0.037 (0.081)	—	—
$\sigma_e (\sigma_h)$ for CB tail ( $\text{cm}^2$ )	$7 \times 10^{-16}$ ( $7 \times 10^{-16}$ )	$1 \times 10^{-12}$ ( $1 \times 10^{-12}$ )	$7 \times 10^{-16}$ ( $7 \times 10^{-16}$ )	—	—
$\sigma_e (\sigma_h)$ for VB tail ( $\text{cm}^2$ )	$7 \times 10^{-16}$ ( $7 \times 10^{-16}$ )	$1 \times 10^{-14}$ ( $1 \times 10^{-14}$ )	$7 \times 10^{-16}$ ( $7 \times 10^{-16}$ )	—	—
Maximum A-like Gaussian state density ( $\text{cm}^{-3}/\text{eV}$ )	$1.4 \times 10^{19}$	$1.0 \times 10^{17}$	$1.3 \times 10^{20}$	—	—
Maximum D-like Gaussian state density ( $\text{cm}^{-3}/\text{eV}$ )	$1.4 \times 10^{19}$	$1.0 \times 10^{17}$	$1.3 \times 10^{20}$	—	—
Specific energy of Gaussian peak for donor (eV)	1.10	0.725	0.50	—	—
Specific energy of Gaussian peak for acceptor (eV)	1.20	1.025	0.60	—	—
Standard deviation of Gaussian for donor (eV)	0.21	0.10	0.21	—	—
Standard deviation of Gaussian for acceptor (eV)	0.21	0.10	0.21	—	—
$\sigma_e (\sigma_h)$ for A-like Gaussian state ( $\text{cm}^2$ )	$3 \times 10^{-15}$ ( $3 \times 10^{-14}$ )	$1 \times 10^{-12}$ ( $1 \times 10^{-12}$ )	$3 \times 10^{-15}$ ( $3 \times 10^{-14}$ )	—	—
$\sigma_e (\sigma_h)$ for D-like Gaussian state ( $\text{cm}^2$ )	$3 \times 10^{-14}$ ( $3 \times 10^{-15}$ )	$1 \times 10^{-14}$ ( $1 \times 10^{-14}$ )	$3 \times 10^{-14}$ ( $3 \times 10^{-15}$ )	—	—

better discussion. When compared, the front and back contacts, optical properties,  $\text{P}^+$ -a-Si, N-c-Si, and  $\text{N}^+$ -a-Si layers are all identical for both types of solar cells.

To focus on studying the properties of the homo–hetero junctions solar cell, neither reflection nor absorption in the transparent conductive oxide film was considered. Both the front and back contacts were assumed to be flatband, as other models [2], [21]. For a-Si layers, both acceptor-like and donor-like states consisting of exponential band tail states and Gaussian gap states were taken into account. The detailed electric parameters of all a-Si layers were mainly set as default values in AFORS-HET while considering a rather accurate DOS distribution that has been presented in our previous work [22]. The doping concentration of the a-Si emitter is  $7.5 \times 10^{18} \text{ cm}^{-3}$ , by keeping the Fermi level 330 meV away from the valence band. The c-Si layers were selected as the c-Si model so that ionized impurity scattering effect and shrink of energy gap varying with doping concentration are included. The DOS distribution in the front a-Si/c-Si interface was assumed to be Gaussian distributed, with the peak at the midgap of c-Si [22], [23] and electron/hole capture cross sections ( $\sigma_e/\sigma_h$ ) of  $1 \times 10^{-15} \text{ cm}^2$ . The DOS in the back a-Si/c-Si interface was neglected for convenience. Carrier transport across the a-Si/c-Si interface was described by the thermionic emission model. The surface recombination velocities of electrons and holes on both sides were set as  $1 \times 10^7 \text{ cm} \cdot \text{s}^{-1}$ . More details about the simulation parameters of different layers including the I-a-Si:H layer are shown in Table I and Fig. 1. Note that, in the numer-

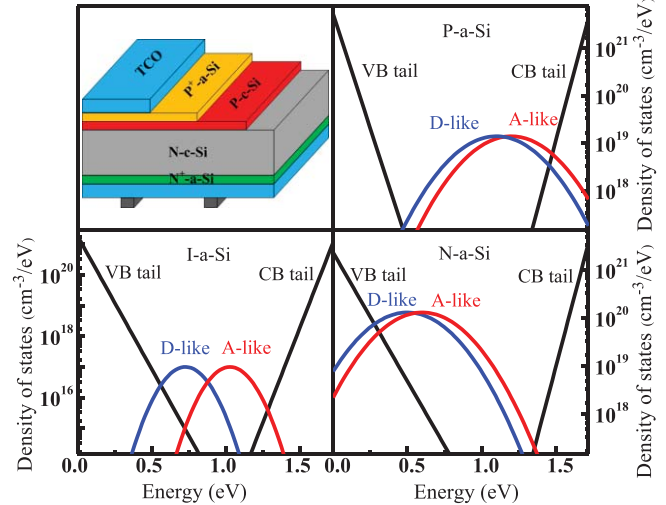


Fig. 1. Schematic diagram of the homo–hetero junctions solar cell and the DOS distributions of the P, I, and N-a-Si layers. CB and VB are conduction band and valence band, respectively; and D-like and A-like represent donor-like and acceptor-like dangling bonds, respectively.

ical simulation, direct band-to-band, Auger, and Shockley–Read–Hall (SRH) recombination process are incorporated. The performances of the solar cells were calculated under AM1.5 solar spectrum ( $100 \text{ mW/cm}^2$ ) condition at room temperature.

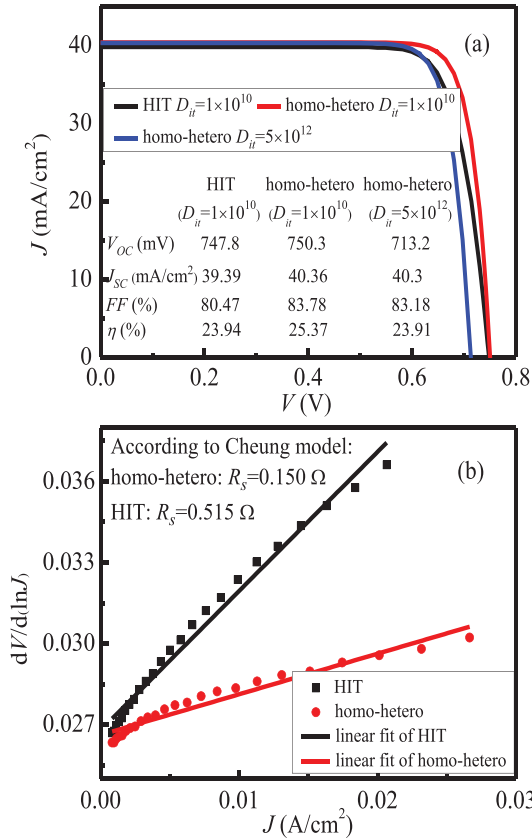


Fig. 2. (a)  $J$ - $V$  characteristics for the homo–hetero junctions solar cell ( $D_{it} = 1.0 \times 10^{10}$  and  $5.0 \times 10^{12} \text{ cm}^{-2}$ , respectively) and HIT ( $D_{it} = 1.0 \times 10^{10} \text{ cm}^{-2}$ ) solar cell under AM1.5 illumination. (b) Plots of  $dV/d(\ln J)$  versus  $J$  extracted from the forward-bias dark  $J$ - $V$  characteristics of the homo–hetero junctions solar cell and HIT solar cell (with  $D_{it} = 1.0 \times 10^{10} \text{ cm}^{-2}$ ).

### III. SIMULATION RESULTS AND DISCUSSION

#### A. Comparison of Solar Cells Performance

Fig. 2(a) shows the current density versus voltage ( $J$ - $V$ ) curve of the HIT solar cell with excellent passivation whose total interfacial DOS ( $D_{it}$ ) is  $1.0 \times 10^{10} \text{ cm}^{-2}$ , and the homo–hetero junctions solar cells with  $D_{it} = 1.0 \times 10^{10} \text{ cm}^{-2}$  and  $5.0 \times 10^{12} \text{ cm}^{-2}$ , under AM1.5 illumination. The doping concentration and thickness of the P-c-Si layer are  $5 \times 10^{18} \text{ cm}^{-3}$  and 10 nm, respectively, which can be easily realized by plasma immersion ion implantation [24], [25]. It is exciting that, due to the obvious better FF, the conversion efficiency ( $\eta$ ) of the homo–hetero junctions solar cell exhibits 1.43% absolute higher than that of the HIT solar cell when they have the identical  $D_{it}$  ( $1.0 \times 10^{10} \text{ cm}^{-2}$ ), reaching as high as 25.37%. Moreover, with the advantage of FF, even if the  $D_{it}$  of the homo–hetero junctions solar cell is 500 folds (with  $D_{it} = 5.0 \times 10^{12} \text{ cm}^{-2}$ ) higher than that of the HIT solar cell (with  $D_{it} = 1.0 \times 10^{10} \text{ cm}^{-2}$ ), they still show comparable efficiencies. We ascribe the inferior FF of the HIT solar cell to the insertion of the I-a-Si layer, since intrinsic a-Si layer often acts as a transport barrier, which will result in high resistance [12], [14]. To confirm this, we have extracted  $dV/d(\ln J)$  versus  $J$  from the forward-bias dark  $J$ - $V$  characteristics of the homo–hetero junctions and HIT

solar cells, plotted in Fig. 2(b). According to the widely accepted calculation model by Cheung *et al.*, based on the thermionic emission theory, we can obtain [26], [27]

$$\frac{dV}{d(\ln J)} = R_s A_{\text{eff}} J + n \left( \frac{k_B T}{q} \right) \quad (1)$$

where  $R_s$  is the series resistance,  $A_{\text{eff}}$  the effective area of the solar cell,  $q$  the electronic charge,  $k_B$  the Boltzmann constant,  $T$  the absolute temperature in kelvin, and  $n$  the ideality diode factor. Considering  $A_{\text{eff}}$  as the unit area, thus, a plot of  $dV/d(\ln J)$  versus  $J$  will give  $R_s$  as the slope. We have made a linear fit of  $dV/d(\ln J)$  versus  $J$ , giving the slope 0.150 and 0.515 for the homo–hetero junctions and HIT solar cells, respectively. Therefore, the  $R_s$  of the homo–hetero junctions solar cell is  $0.150 \Omega$ , indeed smaller than that of the HIT solar cell whose  $R_s$  is  $0.515 \Omega$ . Regarding the open-circuit voltage ( $V_{OC}$ ), relatively higher result is obtained when compared with some real devices [28], [29], which is due to neglecting the rear interface recombination. Furthermore, we note that the  $V_{OC}$  for the homo–hetero junctions solar cell and HIT solar cell can reach as high as 766.2 and 761.3 mV, respectively, as the thickness of the N-c-Si wafer is reduced to  $98 \mu\text{m}$  which is adopted by Panasonic.

#### B. Effect of Inserting a P-c-Si Layer

From the above results, we understand that high-efficiency solar cells can be obtained with the homo–hetero junctions structure. Therefore, to get a further insight into the physical aspects and properties of the homo–hetero junctions solar cell is important. We have investigated the influence of inserting a P-c-Si layer between the P<sup>+</sup>-a-Si emitter and N-c-Si substrate on the solar cell performance. Fig. 3 presents the dependence of the open-circuit voltage  $V_{OC}$ , short-circuit current density  $J_{SC}$ , fill factor FF, and conversion efficiency  $\eta$  on the doping concentration  $N_D$  and thickness of the P-c-Si layer. The  $N_D$  varies from  $1 \times 10^{17}$  to  $5 \times 10^{18} \text{ cm}^{-3}$ , and heavier  $N_D$  (e.g.,  $1 \times 10^{19} \text{ cm}^{-3}$ ) was not discussed in this paper due to the fact that Fermi energy has come into the valence band, thereby the Fermi–Dirac statistic may need to be considered, which has not been incorporated into the software yet. With the increase of the layer thickness, the following can be observed:

- 1)  $V_{OC}$  first rises, and then nearly preserves the same, as the layer thickness is larger than 10 nm.
- 2)  $J_{SC}$  exhibits an increase at the beginning, and then linearly drops down.
- 3) FF changes a little.
- 4)  $\eta$  also behaves to increase first, and starts to decrease at a thickness of 10 nm.

Therefore, 10 nm will be adopted as the optimum P-c-Si layer thickness for further investigation.

With regard to  $N_D$ , higher  $N_D$  leads to lower  $J_{SC}$ , which is more striking at larger P-c-Si layer thickness. These behaviors can be explained from three aspects:

- 1) Ionized impurity scattering and carrier–carrier scattering are enhanced with increasing the  $N_D$ , which leads to the

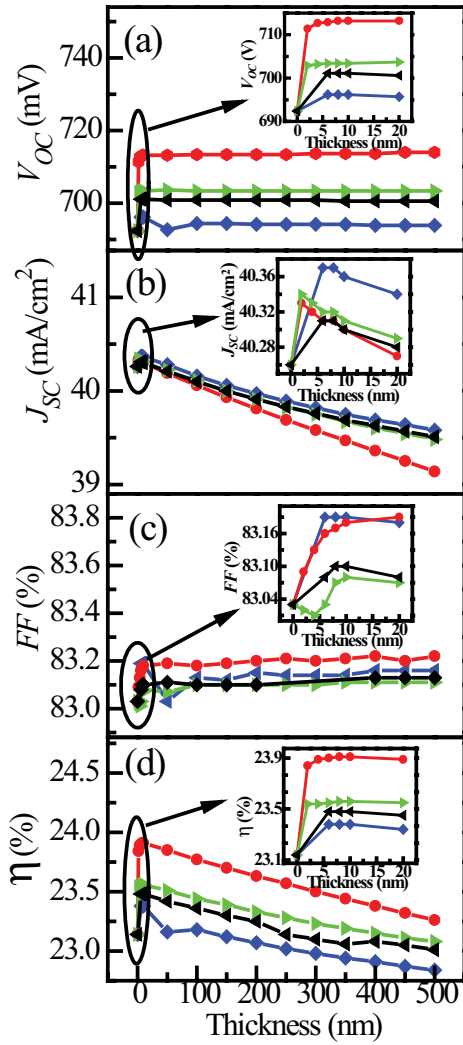


Fig. 3. Effects of the doping concentration as well as the thickness of the P-c-Si layer on (a) Open-circuit voltage ( $V_{OC}$ ). (b) Short-circuit current density ( $J_{SC}$ ). (c) Fill factor (FF), and (d) Conversion efficiency ( $\eta$ ) for the homo-hetero junctions solar cell. The curves in red, green, black, and blue colors represent the doping concentration  $N_D$  of  $5 \times 10^{18}$ ,  $1 \times 10^{18}$ ,  $5 \times 10^{17}$ , and  $1 \times 10^{17} \text{ cm}^{-3}$ , respectively.

reduced electron/hole mobility as listed in Table II, thus recombination probability increases.

- 2) Auger recombination is also enhanced when increasing the  $N_D$ . We have extracted the values at the position of 10 nm and found that it increases from  $1.51 \times 10^{19} \text{ cm}^{-3}/\text{s}$  to  $1.49 \times 10^{20} \text{ cm}^{-3}/\text{s}$  while  $N_D$  rises from  $1 \times 10^{17} \text{ cm}^{-3}$  to  $5 \times 10^{18} \text{ cm}^{-3}$ .
- 3) More electrons and holes will be trapped and recombined at larger layer thickness.

It is interesting that despite these negative effects, the  $V_{OC}$  increases in proportion to the  $N_D$ , and high  $\eta$  tends to prefer rather high doping concentration with a small thickness of the P-c-Si layer. Here, it is worth mentioning that we have also taken into account the influence of an increased defect density in the heavily doped P-c-Si layer on solar cell performance. With the assumption that the defect density increases proportionally with the  $N_D$  [30] (see Table II), the  $V_{OC}$ ,  $J_{SC}$ , FF, and  $\eta$  maintain the same as those without considering

TABLE II  
INFLUENCE OF THE DOPING CONCENTRATION IN THE P-c-Si LAYER ON  
THE ELECTRON/HOLE MOBILITY, AUGER RECOMBINATION RATE AT  
THE POSITION OF 10 NM, ENERGY GAP, AND EMMITTER  
SATURATION CURRENT DENSITY  $J_{0e}$

$N_D$ ( $\text{cm}^{-3}$ )	$1 \times 10^{17}$	$5 \times 10^{17}$	$1 \times 10^{18}$	$5 \times 10^{18}$
Electron mobility ( $\text{cm}^2/\text{V}\cdot\text{s}$ )	672.0	405.4	328.6	225.2
Hole mobility ( $\text{cm}^2/\text{V}\cdot\text{s}$ )	323.1	214.4	170.3	96.39
Auger recombination ( $\text{cm}^{-3}/\text{s}$ )	$1.51 \times 10^{19}$	$2.43 \times 10^{19}$	$3.43 \times 10^{19}$	$1.49 \times 10^{20}$
Energy gap (eV)	1.124	1.106	1.096	1.074
Defect density ( $\text{cm}^{-3}$ )	$1 \times 10^{10}$	$5 \times 10^{10}$	$1 \times 10^{11}$	$5 \times 10^{11}$
$J_{0e}s$ ( $\text{fA}/\text{cm}^2$ )	54.85	40.95	38.16	26.43

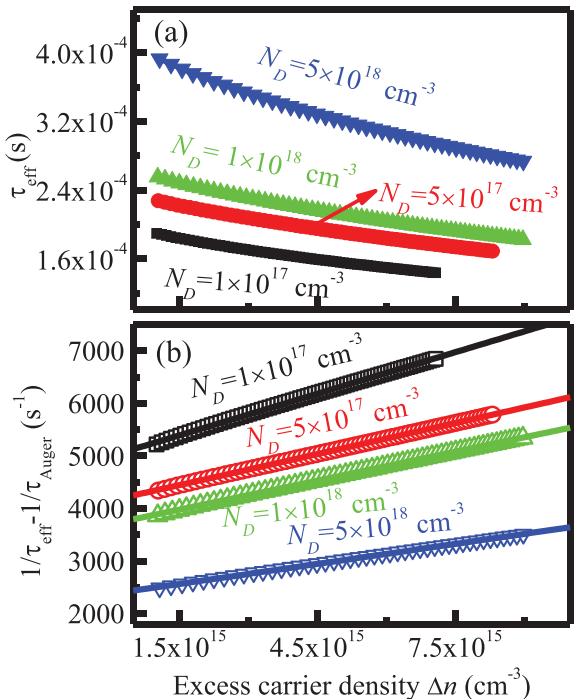


Fig. 4. Calculated effective carrier lifetime and Auger-corrected inverse carrier lifetime versus excess carrier density as a function of doping concentration in the P-c-Si layer.

this effect for the solar cells with a 10-nm P-c-Si layer, which can be ascribed to that the layer thickness is thin enough to neglect the increased defect density.

To further understand the influence of  $N_D$  on cell properties, the injection-dependent effective lifetime ( $\tau_{eff}$ ) of a symmetric structure of  $P^+$ -a-Si/P-c-Si/N-c-Si substrate/P-c-Si/P<sup>+</sup>-a-Si has been calculated by quasi-steady-state photoconductivity method utilizing AFORS-HET, shown in Fig. 4. Moreover, through plotting the inverse  $\tau_{eff}$  reduced by the inverse Auger carrier lifetime ( $\tau_{Auger}$ ) versus the excess carrier density ( $\Delta n$ ), the emitter saturation current density ( $J_{0e}$ ) can be extracted based on the following formulas [31]

$$\frac{1}{\tau_{eff}} - \frac{1}{\tau_{Auger}} = \frac{1}{\tau_{SRH}} + \frac{2J_{0e}}{qn_i^2 W} (N_{dop} + \Delta n) \quad (2)$$

and  $\tau_{Auger}$  can be written as

$$\tau_{\text{Auger}} = \frac{\Delta n}{[C_n(\Delta n + N_{\text{dop}}) + C_p \Delta n][(N_{\text{dop}} + \Delta n)\Delta n - N_C N_V \exp(-E_g/kT)]} \quad (3)$$

where  $C_n$  and  $C_p$  are the Auger coefficients for electrons and holes, respectively;  $\tau_{\text{SRH}}$  is the bulk lifetime considering the SRH recombination;  $q$  is the elementary charge;  $n_i$  represents the intrinsic carrier density;  $W$  denotes the thickness of the wafer;  $E_g$  represents the energy gap;  $N_{\text{dop}}$  is the doping concentration of the substrate; and  $N_C$  and  $N_V$  are the effective DOS in the conduction band and valence band, respectively. Therefore, we can obtain  $J_{0e}$  from the slope of  $1/\tau_{\text{eff}} - 1/\tau_{\text{Auger}}$  versus  $\Delta n$ , listed in Table II. It is amazing that the  $J_{0e}$  reduces with increasing the  $N_D$ , despite the enhanced recombination in the P-c-Si layer as discussed above. In general, for a traditional homojunction solar cell, the  $J_{0e}$  rises when increasing the  $N_D$  (or decreasing the sheet resistance) [32]. The difference may be attributed to that the interface recombination plays a dominant role for our homo-hetero junctions solar cell compared with the bulk recombination in the P-c-Si layer, and the interface recombination is reduced with a heavier  $N_D$ . Fig. 4 also reveals that the  $\tau_{\text{eff}}$  increases when increasing the  $N_D$ , which suggests that an improved field-effect passivation exists [33].

### C. Field-Effect Passivation

We extracted the band diagram, electric field, as well as the free electron density as a function of position from the numerical simulation software to further understand the field-effect passivation mechanism in our homo-hetero junctions device, depicted in Fig. 5. In the band diagram, there are obvious differences on the energy band between the a-Si emitter and c-Si substrate with different doping concentrations of the P-c-Si layer. Firstly, the valence band gradually exhibits a discontinuity within the homojunction when increasing the  $N_D$ , due to the bandgap narrowing of the P-c-Si layer, as presented in Table II. As a result, the band offset in the valence band ( $\Delta E_V$ ) for the homojunction reaches 0.05 eV while the  $N_D$  of the P-c-Si layer is  $5 \times 10^{18} \text{ cm}^{-3}$ . Secondly, heavier doping concentration induces more rapid change of the energy band near the c-Si substrate, which indicates stronger electric field at the given position, as confirmed in Fig. 5(b). It is well known that “a band bending at the silicon surface through the creation of an electric field can provide an energetic barrier to charge accumulation at the interface, and then the recombination rate will be strongly reduced as electron/hole concentrations are unbalanced” [29], which is the mechanism of field-effect passivation. For the homo-hetero junctions solar cell, due to the gradually enhanced electric field within the homojunction with increasing  $N_D$ , thus, better field-effect passivation, the electrons will gradually repel away from the heterointerface, verified in Fig. 5(c). Therefore, the recombination rate at the interface is reduced with a heavier  $N_D$ , resulting in the improvement of both  $V_{\text{OC}}$  and  $J_{0e}$ .

Here, it is worth mentioning that the homo-hetero junctions solar cell can also be understood as an ultrathin doped conventional homojunction passivated by a heterojunction due to its field-effect passivation, in order to suppress contact

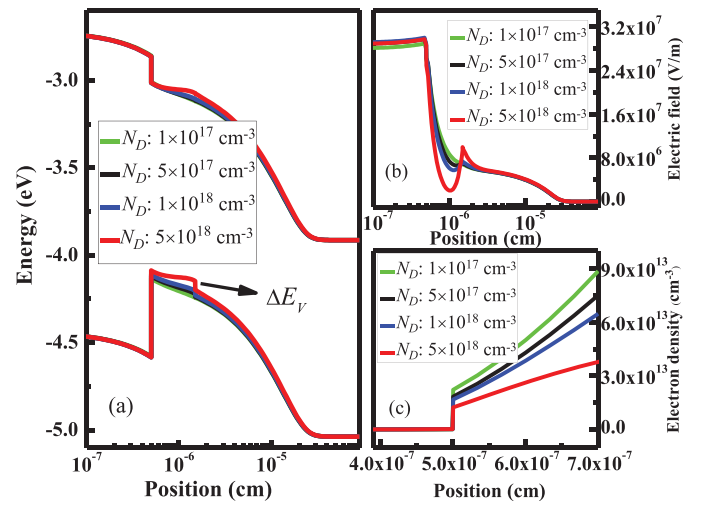


Fig. 5. (a) Energy band diagram. (b) Electric field. (c) Free electron density under AM1.5 illumination as a function of position under different doping concentrations in the P-c-Si layer.

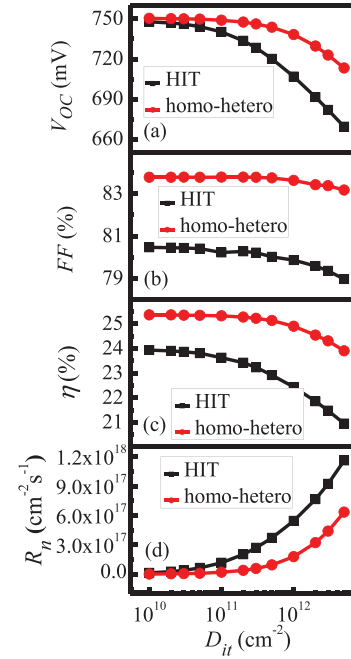


Fig. 6. Comparisons of (a)  $V_{\text{OC}}$ , (b) FF, (c)  $\eta$ , and (d)  $R_n$  between the homo-hetero junctions solar cell and HIT solar cell varying with the  $D_{\text{it}}$ . Thereinto, the doping concentration and thickness of the P-c-Si layer are  $5 \times 10^{18} \text{ cm}^{-3}$  and  $10 \text{ nm}$ , respectively.

recombination, and thus enhance the  $V_{\text{OC}}$ . Besides, the larger energy gap of the a-Si with respect to that of the c-Si, is also a benefit to obtain a high  $V_{\text{OC}}$ .

### D. Better Tolerance for Interfacial DOS

The comparisons of the  $V_{\text{OC}}$ , FF, and  $\eta$  between the HIT and homo-hetero junctions solar cells as a function of the  $D_{\text{it}}$  are plotted in Fig. 6(a), (b), and (c). Here, the doping concentration and thickness of the P-c-Si layer are  $5 \times 10^{18} \text{ cm}^{-3}$  and

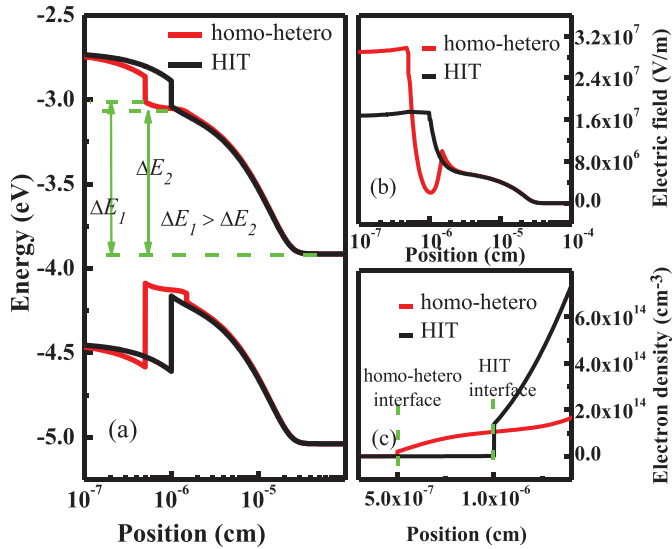


Fig. 7. Comparisons of (a) Energy band. (b) Electric field. (c) Free electron density between the homo–hetero junctions solar cell and HIT solar cell as a function of position.

10 nm, respectively. It is important that the homo–hetero junctions solar cell shows a higher  $V_{\text{OC}}$ , FF, and  $\eta$  than the HIT solar cell at any given  $D_{\text{it}}$ . Moreover, the  $V_{\text{OC}}$  of the homo–hetero junctions solar cell performs less sensitive to the  $D_{\text{it}}$ . In contrast, the  $V_{\text{OC}}$  of the HIT solar cell decays sharply with increasing  $D_{\text{it}}$ , which is consistent with the previous study [15]. As a result, even though the  $D_{\text{it}}$  of the homo–hetero junctions solar cell is 10 times larger than that of the HIT solar cell, they still have a comparable  $V_{\text{OC}}$ . These results are interesting, since there is a highly doped P-c-Si layer, which is a high recombination layer for photogenerated carriers in the homo–hetero junctions solar cell. We believe that the better  $V_{\text{OC}}$  for the homo–hetero junctions solar cell can be understood from the interfacial recombination. According to the calculation method in the AFORS-HET [34], the electron recombination rate ( $R_n$ ) at the front a-Si/c-Si interface varying with the  $D_{\text{it}}$  can be obtained, which is depicted in Fig. 6(d). When  $D_{\text{it}} < 5.0 \times 10^{10} \text{ cm}^{-2}$ , there is not a big difference of the  $R_n$  between the homo–hetero junctions solar cell and HIT solar cell, since the interfacial recombination is not an important factor to restrain the cell properties in such a low  $D_{\text{it}}$ . In this case, the better  $\eta$  for the homo–hetero junctions solar cell is solely attributed to its higher FF. When  $D_{\text{it}} > 5.0 \times 10^{10} \text{ cm}^{-2}$ , the  $R_n$  of the HIT solar cell dramatically rises with the increase of the  $D_{\text{it}}$ , whereas, the  $R_n$  of the homo–hetero junctions solar cell is less sensitive to the  $D_{\text{it}}$ , resulting in the obvious higher  $V_{\text{OC}}$ . Note that, with the benefit of a better tolerance for the  $D_{\text{it}}$ , rigorous process to restrain the  $D_{\text{it}}$  as low as possible becomes not such important, which is easier to make the homo–hetero junctions solar cell shows in a stable level in mass production.

In order to get further insight into the better tolerance for the  $D_{\text{it}}$  of the homo–hetero junctions solar cell, the energy band, electric field, and free electron density as a function of position have been investigated, which is illustrated in Fig. 7. The energy band of the homo–hetero junctions solar

cell changes more rapidly in the c-Si substrate with respect to that of the HIT solar cell. In addition, less potential drop in the a-Si layer is observed due to not inserting an I-a-Si layer, leading to the energy barrier on the c-Si side ( $\Delta E_1$ ) higher than that ( $\Delta E_2$ ) of the HIT solar cell. Correspondingly, the electric field on the c-Si substrate side and in the a-Si layer is higher. Though the band offset in the valence band within the heterojunction is bigger for the homo–hetero junctions solar cell, which results in the accumulation of holes on the heterointerface (the result is not presented), the electron density is greatly reduced on the interface owing to the field-effect passivation from the homojunction. Therefore, the  $R_n$  of the homo–hetero junctions solar cell is lower than that of the HIT solar cell at any given  $D_{\text{it}}$ , and its  $V_{\text{OC}}$  is less sensitive to the  $D_{\text{it}}$ .

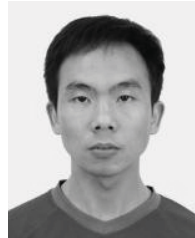
#### IV. CONCLUSION

The physical aspects and properties of a novel solar cell structure of  $P^+$ -a-Si/P-c-Si/N-c-Si/ $N^+$ -a-Si were studied in detail utilizing AFORS-HET software as numerical simulation. We were excited to find that the FF of the homo–hetero junctions solar cell is higher than that of the HIT solar cell due to the replacement of the I-a-Si:H layer, resulting in almost the same  $\eta$  even if the  $D_{\text{it}}$  of the homo–hetero junctions solar cell is 500-folds larger. In order to further understand the properties and benefits of the homo–hetero junctions solar cell, we investigated the performances of the solar cells varying with the  $N_D$  and thickness of the P-c-Si layer. Though the recombination in the layer increases when increasing the  $N_D$ , high  $\eta$  can be obtained with a rather heavy  $N_D$  and thin layer thickness. Furthermore, through investigating the energy band, electric field, and electron density, we found that it is appropriate to apply field-effect passivation theory to explain the interesting behaviors that the  $V_{\text{OC}}$  increases and  $J_{0e}$  drops when increasing the  $N_D$ . The field-effect passivation can also be applied to understand the phenomenon that the  $R_n$  of the homo–hetero junctions solar cell exhibits less sensitive to the  $D_{\text{it}}$ , as compared to the HIT solar cell. Therefore, with the advantage of better tolerance for the  $D_{\text{it}}$ , the  $V_{\text{OC}}$  of the homo–hetero junctions solar cell is still comparable to that of the HIT solar cell when its  $D_{\text{it}}$  is 10 times larger. In conclusion, we believe that the homo–hetero junctions scheme opens a new opportunity for high-efficiency crystalline silicon solar cells.

#### REFERENCES

- [1] Y. Tsunomura, Y. Yoshimine, M. Taguchi, T. Baba, T. Kinoshita, H. Kanno, H. Sakata, E. Maruyama, and M. Tanaka, “Twenty-two percent efficiency HIT solar cell,” *Solar Energy Mater. Solar Cells*, vol. 93, pp. 670–673, Jun. 2009.
- [2] L. Zhao, C. L. Zhou, H. L. Li, H. W. Diao, and W. J. Wang, “Design optimization of bifacial HIT solar cells on p-type silicon substrates by simulation,” *Solar Energy Mater. Solar Cells*, vol. 92, pp. 673–681, Jun. 2008.
- [3] S. D. Wolf, “Intrinsic and doped a-Si:H/c-Si interface passivation,” in *Physics and Technology of Amorphous-Crystalline Heterostructure Silicon Solar Cells*, G. J. Wilfried, H. M. van Sark, L. Korte, and F. Roca, Eds. New York, NY, USA: Springer-Verlag, 2011, pp. 233–234.
- [4] H. Fujiwara and M. Kondo, “Impact of epitaxial growth at the heterointerface of a-Si:H/c-Si solar cells,” *Appl. Phys. Lett.*, vol. 90, p. 013503, Jan. 2007.

- [5] H. Fujiwara, H. Sai, and M. Kondo, "Crystalline Si heterojunction solar cells with the double heterostructure of hydrogenated amorphous silicon oxide," *Jpn. J. Appl. Phys.*, vol. 48, p. 064506, Jun. 2009.
- [6] S. Olibet, E. Vallat-Sauvain, L. Fesquet, C. Monachon, A. Hessler-Wyser, J. Damon-Lacoste, S. De Wolf, and C. Ballif, "Properties of interfaces in amorphous/crystalline silicon heterojunctions," *Phys. Status Solidi A*, vol. 207, pp. 651–656, Jan. 2010.
- [7] L. Korte, E. Conrad, H. Angermann, R. Stangl, and M. Schmidt, "Advances in a-Si:H/c-Si heterojunction solar cell fabrication and characterization," *Solar Energy Mater. Solar Cells*, vol. 93, pp. 905–910, Jun. 2009.
- [8] S. Miyajima, J. Irikawa, A. Yamada, and M. Konagai, "High-quality nanocrystalline cubic silicon carbide emitter for crystalline silicon heterojunction solar cells," *Appl. Phys. Lett.*, vol. 97, p. 023504, Jul. 2010.
- [9] D. Munoz, A. S. Ozanne, S. Harrison, A. Danel, F. Souche, C. Denis, A. Favier, T. Desrues, S. M. de Nicolas, N. Nguyen, P. E. Hickel, P. Mur, T. Salvetat, H. Moriceau, Y. Le-Tiec, M. S. Kang, K. M. Kim, R. Janin, C. Pesenti, D. Blin, T. Nolan, I. Kashkoush, and P. J. Ribeyron, "Toward high efficiency on full wafer a-Si:H/c-Si heterojunction solar cells: 19.6% on 148cm<sup>2</sup>," in *Proc. 35th IEEE Photovolt. Specialists Conf.*, Jun. 2010, pp. 39–43.
- [10] M. Tucci and G. de Cesare, "17% efficiency heterostructure solar cell based on p-type crystalline silicon," *J. Non-Cryst. Solids*, vol. 338, pp. 663–667, Jun. 2004.
- [11] Q. Wang, M. R. Page, E. Iwaniczko, Y. Q. Xu, L. Roybal, R. Bauer, B. To, H. C. Yuan, A. Duda, and Y. F. Yan, "Crystal silicon heterojunction solar cells by hot-wire CVD," in *Proc. 33rd IEEE Photovolt. Specialists Conf.*, May 2008, pp. 453–457.
- [12] M. Zeman and D. Zhang, "Heterojunction silicon based solar cells," in *Physics and Technology of Amorphous-Crystalline Heterostructure Silicon Solar Cells*, G. J. Wilfried, H. M. van Sark, L. Korte, and F. Roca, Eds. New York, NY, USA: Springer-Verlag, 2011, p. 23.
- [13] M. Rahmouni, A. Datta, P. Chatterjee, J. Damon-Lacoste, C. Ballif, and P. Rocai Cabarrocas, "Carrier transport and sensitivity issues in heterojunction with intrinsic thin layer solar cells on N-type crystalline silicon: A computer simulation study," *J. Appl. Phys.*, vol. 107, p. 054521, Mar. 2010.
- [14] G. Garcia-Belmonte, J. García-Cañadas, I. Mora-Seró, J. Bisquert, C. Voz, J. Puigdollers, and R. Alcubilla, "Effect of buffer layer on minority carrier lifetime and series resistance of bifacial heterojunction silicon solar cells analyzed by impedance spectroscopy," *Thin Solid Films*, vol. 514, pp. 254–257, Aug. 2006.
- [15] A. Datta, M. Rahmouni, M. Nath, R. Boubekri, P. R. I. Cabarrocas, and P. Chatterjee, "Insights gained from computer modeling of heterojunction with intrinsic thin layer 'HIT' solar cells," *Solar Energy Mater. Solar Cells*, vol. 94, pp. 1457–1462, Sep. 2010.
- [16] A. Das, D. S. Kim, K. Nakayashiki, B. Rounsville, V. Meemongkolkiat, and A. Rohatgi, "Boron diffusion with boric acid for high efficiency silicon solar cells," *J. Electrochem. Soc.*, vol. 157, p. 684, May 2010.
- [17] X. Gu, X. G. Yu, and D. R. Yang, "Efficiency improvement crystalline silicon solar cells with a back-surface field produced by boron and aluminum co-doping," *Scripta Mater.*, vol. 66, pp. 394–397, Mar. 2012.
- [18] F. Granek, M. Hermle, D. M. Huljic, O. Schultz-Wittmann, and S. W. Glunz, "Enhanced lateral current transport via the front N+diffused layer of n-type high-efficiency back-junction back-contact silicon solar cells," *Prog. Photovolt. Res. Appl.*, vol. 17, pp. 47–56, Jan. 2009.
- [19] I. M. Dharmadasa, "Third generation multi-layer tandem solar cells for achieving high conversion efficiencies," *Solar Energy Mater. Solar Cells*, vol. 85, pp. 293–300, Jan. 2005.
- [20] N.-P. Harder, "Heterojunction solar cell with absorber having an integrated doping profile," U.S. Patent 0174374A1, Jul. 21, 2011.
- [21] J. Q. Wang, F. Y. Meng, Z. D. Fang, and Q. H. Ye, "Investigation of a-Si (N+)/c-Si (P) hetero-junction solar cell through AFORS-HET simulation," *Surf. Inter. Anal.*, vol. 43, pp. 1211–1217, Sep. 2011.
- [22] X. Hua, Z. P. Li, W. Z. Shen, G. Y. Xiong, X. S. Wang, and L. J. Zhang, "Mechanism of trapping effect in heterojunction with intrinsic thin-layer solar cells: Effect of density of defect states," *IEEE Trans. Electron Devices*, vol. 59, no. 5, pp. 1227–1235, May 2012.
- [23] C. Leendertz, R. Stangl, T. F. Schulze, M. Schmidt, and L. Korte, "A recombination model for a-Si:H/c-Si heterostructures," *Phys. Status Solidi C*, vol. 7, pp. 1005–1010, Jan. 2010.
- [24] F. Torregrosa, H. Etienne, G. Mathieu, and L. Roux, "Down to 2 nm ultra shallow junctions: Fabrication by IBS plasma immersion ion implantation prototype pulsion," in *Proc. AIP Conf.*, vol. 866, Jun. 2006, pp. 609–613.
- [25] F. Torregrosa, C. Laviron, H. Faik, D. Barakel, F. Milesi, and S. Beccaccia, "Realization of ultra shallow junctions by PIII: Application to solar cells," *Surf. Coatings Technol.*, vol. 186, pp. 93–98, Aug. 2004.
- [26] S. K. Cheung and N. W. Cheung, "Extraction of Schottky diode parameters from forward current-voltage characteristics," *Appl. Phys. Lett.*, vol. 49, p. 85, May, 1986.
- [27] A. Sertap Kavasoglu, O. Birgi, N. Kavasoglu, G. Oylumluoglu, A. Osman Kodolbas, R. Kangi, and O. Yilmaz, "Electrical characterization of a-Si:H(n)/c-Si(p) structure," *J. Alloys Compounds*, vol. 509, pp. 9394–9398, Sep. 2011.
- [28] Z. C. Holman, A. Descouedres, L. Barraud, F. Z. Fernandez, J. P. Seif, S. De Wolf, and C. Ballif, "Current losses at the front of silicon heterojunction solar cells," *IEEE J. Photovolt.*, vol. 2, no. 1, pp. 7–15, Jan. 2012.
- [29] S. M. De Nicolás, "a-Si:H/c-Si heterojunction solar cells: Back side assessment and improvement," Ph.D. dissertation, Inst. Nat. DEL Énergie Solaire, Univ. Paris-SUD, Paris, France, 2012.
- [30] J. Schmidt and K. Bothe, "Structure and transformation of the metastable boron- and oxygen-related defect center in crystalline silicon," *Phys. Rev. B*, vol. 69, p. 024107, Jan. 2004.
- [31] D. E. Kane and R. M. Swanson, "Measurement of the emitter saturation current by a contactless photocconductivity decay method," in *Proc. 18th IEEE Photovolt. Specialists Conf.*, Jan. 1985, pp. 578–581.
- [32] P. Saint-Cast, A. Richter, E. Billot, M. Hofmann, J. Benick, J. Rentsch, R. Preu, and S. W. Glunz, "Very low surface recombination velocity of boron doped emitter passivated with plasma-enhanced chemical-vapor-deposited AlO<sub>x</sub> layers," *Thin Solid Films*, vol. 522, pp. 336–339, Nov. 2012.
- [33] C. Leendertz, N. Mingirulli, T. F. Schulze, J. P. Kleider, B. Rech, and L. Korte, "Discerning passivation mechanisms at a-Si:H/c-Si interfaces by means of photoconductance measurements," *Appl. Phys. Lett.*, vol. 98, p. 202108, May, 2011.
- [34] R. Stangl, C. Leendertz, and J. Haschke, "Numerical simulation of solar cells and solar cell characterization methods: The open-source on demand program AFORS-HET," in *Solar Energy*, R. D. Rugescu, Ed. Rijeka, Croatia: InTech, 2010, pp. 331–339.



**Sihua Zhong** is currently pursuing the Ph.D. degree with the Department of Physics, Shanghai Jiao Tong University, Shanghai, China.

His current research interests include solar energy materials and solar cells.



**Xia Hua** was born in Wuxi, China, in 1989. He is currently pursuing the Ph.D. degree with the Department of Physics, Shanghai Jiao Tong University, Shanghai, China.

His current research interests include semiconductor device physics and solar cells.



**Wenzhong Shen** received the Ph.D. degree in semiconductor physics and semiconductor device from Shanghai Institute of Technical Physics, Shanghai, China, in 1995.

He is a Full Professor with the Department of Physics, Shanghai Jiao Tong University, Shanghai.